Exoplanet Characterisation Observatory (EChO)

Assessment Phase Payload Study

Comparison between EChOSim 3.0 and ESA Radiometric model (May 2013)

ECHO-TN-0002-UCL

Issue 1.0

Prepared by: I.P. Waldmann, J. C. Morales, M. Tessenyi, R. Varley Date: 22/08/13

Checked / Approved by: E. Pascale, B. Swinyard, G. Tinetti, V. Coudé du Foresto Date: 23/08/13

DOCUMENT CHANGE DETAILS

Issue	Date	Page	Description Of Change	Comment
0.1	18/06/2013	10	Initial version	
0.2	24/06/2013	10	New figures comparing different binning, updated legends	
0.3	24/06/2013	10	Corrections to text	
0.4	25/06/2013	10	New figures given new wavelength cut offs	
0.5	12/07/2013	10	Added comments from ESA	
0.6	22/08/2013	16	Added additional text, fixed formatting issues	
0.7	27/08/2013	16	Included additional comments	
0.8	28/08/2013	16	Final formatting	
1.0	13/09/2013	All	Implemented addition comments from ESA	

DISTRIBUTION LIST

EChO Payload Consortium				External	
Co-PIs / Science Team Coordinators		Study Engineering Team Working Group Leads		European Space Agency	
✓	Giovanna Tinetti	✓	Paul Eccleston		Luigi Colangeli
	Hans Ulrik Nørgaard-Nielsen	✓	Ranah Irshad	✓	Kate Isaak
	Jean-Philippe Beaulieu	✓	Emanule Pace	✓	Ludovic Puig
	Paul Hartogh	✓	Gianluca Morgante	✓	Martin Linder
	Giusi Micela	✓	Berend Winter		Roger Walker
	Ignasi Ribas	✓	Marc Ferlet		Matthias Ehle
✓	Bruce Swinyard	✓	Mercedes Lopez-Morales		Nicola Rando
	Mark Swain	✓	Vince Coudé du Foresto		
	Tanya Lim	✓	Alberto Adriani		
	Neil Bowles	✓	Jean-Michel Reess		
✓	Enzo Pascale	✓	Marc Ollivier		
	Gillian Wright	✓	Gonzalo Ramos Zapata		
	Graziella Branduardi-Raymont	✓	Neil Bowles		
✓	Marc Ollivier	**Other Engineering Team**			
	Pierre-Olivier Lagage	✓	*Marcell Tessenyi*		
✓	Vince Coudé du Foresto	✓	*Juan Carlos Morales*		
	Athena Coustenis	✓	*Ryan Varley*		
	Emanuele Pace				
	Giuseppe Piccioini				
	Giuseppe Malaguti				
	Alessando Sozzetti				
	Maria Rosa Zapataro Osorio				
	Mercedes Lopez-Morales				
	Enric Palle				
	Christopher Jarchow				
	Denis Grodent				
	Allan Hornstrup				
	Geza Kovacs				
	Pierre Drossart				
	T Encrenaz				
	L Fletcher				
	D Pinfield				
	J Cho				
	F Forget				
✓	I Waldmann				
	P Deroo				
	I Mueller-Wodarg				
	F Selsis				
	O Grasset				
	L Stixrude				
	T Guillot				
	Others…				

TABLE OF CONTENTS

1 PREAMBLE

1.1 PURPOSE & SCOPE

This note compares the performances of the ESA Radiometric Model (ESA-RM) with those of EChOSim. The comparison will be drawn between 55 Cnc e and GJ1214b, the photon and detector limited cases outlined in the MRD.

1.2 APPLICABLE DOCUMENTS

AD #	APPLICABLE DOCUMENT TITLE	DOCUMENT ID	ISSUE / DATE
1			
2			
3			

1.3 REFERENCE DOCUMENTS

RD #	REFERENCE DOCUMENT TITLE	DOCUMENT ID	ISSUE / DATE
1	EChOSim URD		
2	EChOSim SRD		
3	EChO MRD	3.0	
4	Instrument design parameters for EChOSim	ECHO-MO-0003-RAL	

2 INTRODUCTION

In order to show the agreement between the ESA-RM and EChOSim, we present three types of comparisons showing the signal to noise ratio estimated using different settings for both models:

1) ESA-RM run with default parameters and ESA-RM run with EChOSim quantum efficiencies (QEs) and throughputs (TPs). EChOSim parameters (such as QEs and throughput) are periodically updated to reflect the current instrument design specifications.

   Such simulations demonstrate the impact of varying system parameters on the final SNR of the spectrum.

2) Direct comparisons between ESA-RM and EChOSim for two individual planets. These planets represent the limiting cases outlined in the MRD: photon noise limited (55 Cnc e) and detector noise limited (GJ1214b). In addition to the direct comparision between ESA-RM and EChOSim, we also investigate the impact of diffuse emission sources such as Zodi and thermal emissions. This is particularly instructive since Zodi is considered by both models, however thermal emissions are only implemented by EChOSim.

3) A comparison over a range of stellar/planetary types as function of *K* magnitude to check any dependence on *stellar brightness*. We perform this study for various stellar and planetary types. The aim of these simulations is to investigate potential behavioural differences between ESA-RM and EChOSim with respect to the calculation of the astrophysical scene and in particular the host-star star flux.

Note: At the time when the simulations were run, on which this tech note is based, the VIS fibre-fed channel was implemented but not fully tested. We have opted to include this wavelength region in the signal to noise plots in section 3 but is not otherwise referred to. Further note that no pointing jitter effects are assumed for the comparision.

2.1 TEST-CASES: 55CNC E AND GJ1214B

In section 3.1 we compare the performance of EChOSim and ESA-RM using two test cases. The stellar/planetary and orbital parameters used in all simulations are given in table 1. Although effective stellar temperature and log(g) are given as input parameters, EChOSim selects the nearest values from the spectral energy distribution (SED) library. This SED library is the same that is used in the ESA-RM.

Table 1 Planetary and stellar parameters used for simulations in section 3.1

Parameter	**55 Cnc e (HSE)**	**GJ 1214b (WSE)**
Distance (pc)	12.45	13.7
R_{star} ($R_{\odot}$)	0.943	0.21
$T_{eff,star}$ (K)	5250	3020 (3070 adopted)
Log (g)	4.45	4.98
[Fe/H]	0.0	0.0
RA	133.154167	258.829167
DEC	28.33389	4.96389
R_{planet} (R_J)	0.17731	0.2396
M_{planet} (M_J)	0.027	0.020
Albedo	0.1	0.3
Orbital Period (days)	0.934	1.586
Orbital semi-major axis (au)	0.01812	0.01424
Orbital inclination (deg)	82.71 (90.0 adopted)	87.93 (90.0 adopted)
Orbital eccentricity	0.0	0.0
Average molecular weight (kg)	3×10^{-26}	3×10^{-26}
$T_{1,4}$ (s, **computed by EChOSim**)	6333.2 (for i=90 deg)	3333.5 (for i=90 deg)
$T_{eff,planet}$ (K, **computed by EChOSim**)	1778.5	519.9

2.2 RADIOMETRIC MODEL PARAMETERS

The ESA-RM used in this work corresponds to the version of May 2013 (Rad Mod – May 2013.xls). Table 2 summarises the input values used for the ESA-RM. Throughout this document, two different sets are used in general, except otherwise indicated, corresponding to the Standard Model (with parameters as in the original version of the Excel file) and to EChOSim QE & **η** (with parameters comparable to those of EChOSim).

Note on Nmin parameter: EChOSim does not assume a constant and fixed absolute noise floor (Nmin) per detector. It is hence difficult to translate Nmin into meaningful EChOSim equivalent. The only constant noise term present in EChOSim is the detector read-out noise.

In the ESA-RM 'Standard Model', we have set the Nmin parameter to zero (200 given in the original excel file) to allow an adequate comparison between EChOSim and ESA-RM. In the 'EChOSim QE & η'

model we have set Nmin to be the EChOSim assumed read-out noise ranging from 10 – 100 electrons (provided by M. Ferlet's technote).

Table 2 ESA-RM parameters used for simulations in section 3.1

Parameters	ESA-RM Standard Model	ESA-RM EChOSim QE & η
Wavelength range (μm)	0.4-1, 1-5, 5-11, 11-16	0.4-1, 1-5, 5-11, 11-16
Relative Noise Floor (X)	200%, 30%, 30%, 0%	200%, 30%, 30%, 30%
Absolute Noise floor (Nmin)	0, 0, 0, 0	10, 10, 100, 100
QE	60%, 70%, 50%, 50%	60%, 70%, 60%, 60%
Throughput	10%, 25%, 25%, 25%	10%, 28%, 28%, 28%
Resolution	300, 300, 30, 30	300, 300, 30, 30

2.3 ECHOSIM PARAMETERS

Table 3 summarises the EChOSim instrumental input parameters adopted for the models labelled as "Standard EChOSim" throughout this document. Mean values of quantum efficiency and throughput are indicated (figure as a function of wavelength?)

Table 3 EChOSim instrument parameters

Parameters	SWIR	MIR1	MIR2	LWIR	Other
Wave. Range (µm)	2.5 – 5.0	5.0 – 8.5	8.5 – 11.0	11.0 – 16.0	
Det. QE	70%	60%	60%	60%	
Throughput	28%	28%	28%	28%	
Dichroic Emission	3%	3%	3%	0%	
Temp. Optics (K)	45	45	45	45	
Temp. Mirrors (K)					45
Eff. Area (m^2)					1.131
Native Resolution (R)	395	40	115	50	
Final Resolution (R)	300	30	30	30	
Det. Pixel num. X	1000	70	45	65	
Det. Pixel Num. Y	22	12	12	10	
Pixel width (µm)	15	25	25	25	
DC (e pix^{-1} s^{-1})	0.05	1.3	1.3	1.3	
DC temp. (K)	45	7	7	7	
Read noise (e s^{-1})	10.0	100.0	100.0	100.0	
Slit width (pix)	4.77	3.90	3.90	4.18	
Aberration param.	0.55	0.8	0.8	0.9	
Pixel shape Kx	2.575223	1.838698	1.838698	1.453937	
Pixel shape Ky	1.751852	1.250815	1.250815	0.989073	
Eff. Focal Number	3.0	2.6	2.6	2.2	
Eff. Focal length (mm)	3600	3100	3100	2600	
Integration time (s)					20

The aberration parameters (Kax) relate to the Pixel shape parameters Kx and Ky in the following way

$$Kx = \frac{F_{eff}}{\sqrt{(\pi\ Kax\ A_{eff})}}$$

where F_{eff} is the effective focal length and A_{eff} the effective area of the telescope. The PSF is elongated in the spatial direction by $Ky = 1.41 \times Kx$.

Note that in table 3, the 'Temp. Mirrors' parameter describes the telescope temperatures (currently we implement the emission of three separate mirrors), whilst the 'Temp. Optics' parameter accounts for the temperature of the optical bench.

We plot the EChOSim transmission efficiencies in figure 1 for all wavelengths. For the 'EChOSim QE & η' model we adopt the median transmission per detector band (~ 28%), disregarding band edges.

The transmission efficiency profile in figure 1 is compliant with the transmission provided by Mark Ferlet, quoting a transmission range from 20 – 40%. We have opted for a slightly more conservative transmission compared to M. Ferlet's tech note (figure 2 in said tech note). Table 4 summarises the mean transmission efficiencies over the whole bands and excluding dichroic edges.

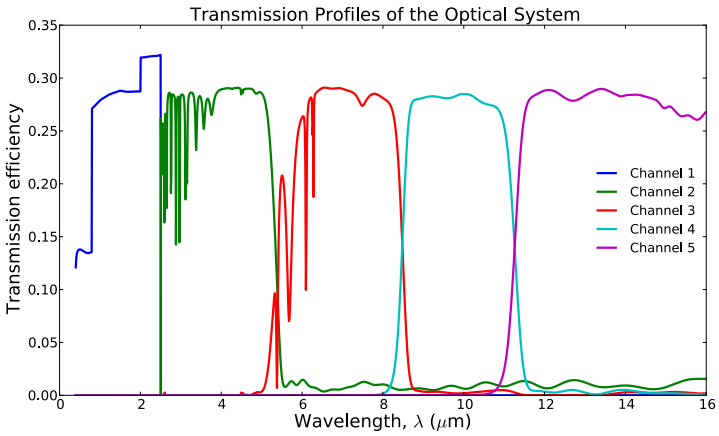

Figure 1: Transmission Profiles of EChOSims optical throughput.

Table 4: Mean transmission efficiencies over the full channel (including dichroic edges) and transmission mean efficiencies over band centres (excluding dichroic edges).

Channel	Transmission mean over band	Transmission mean at centre
VNIR	0.247	0.284
SWIR	0.270	0.289
MIR1	0.258	0.286
MIR2	0.272	0.281
LWIR	0.277	0.280

2.4 CURRENT ECHOSIM ZODI IMPLEMENTATION

The zodiacal light is dominated at short wavelengths (< 3.5 μm) by scattered sunlight and at long wavelengths (> 3.5 μm) by thermal emission from the same dust. In agreement with the MRD (R-PERF-390) we currently adopt a modified version of the JWST-MIRI Zodiacal "model" that is parameterised as follows:

$$Zodi(\lambda) = B_\lambda(5500K)\times 3.5e^{-14} + B_\lambda(270K)\times 3.58e^{-8} \quad W\ m^{-2}\ sr^{-1}\ \mu m^{-1}$$

In the current implementation of EChOSim, the Zodi contributions are not calculated on a per-target basis but we provide three settings to reflect different ecliptic latitudes: minimum (0.9 x Zodi(λ)), average (2.5 x Zodi(λ)), maximum (8.0 x Zodi(λ)). We calculate the Zodi contribution over the pixel solid-angle (which constitutes the Zodi's field of view).

2.5 ECHOSIM BINNING

The spectral resolution ($R = \lambda_c/\Delta\lambda$) of the EChO baseline design exceeds the specified resolutions of R = 300 and R = 30 below and above 5 μm respectively. This requires a binning of the spectrum at the data-reduction stage. Two binning modes are implemented in EChOSim:

Method 1) **constant $\Delta\lambda$**: The wavelength bin size is constant across a given detector focal plane array calculated at the central wavelength of the detector array (λ_c)

Method 2) **constant R**: The wavelength bin size is changing depending on wavelength λ.

A comparision of between both binning types is shown in figure 2. Here one can see that the effect is most prominent in the SWIR channel and has little effect in other channels.

Throughout this document, we have adopted the constant R option, unless otherwise indicated.

Note: The binning is not optimised to account for dichroic overlaps, which results in overly pessimistic SNR at the affected wavelengths.

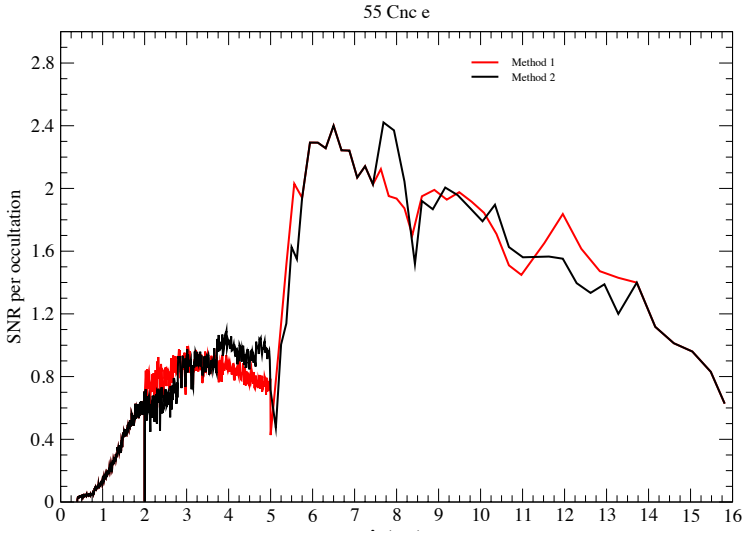

Figure 2. Two binning: constant $\Delta\lambda$ (black), constant R (red).

3 COMPARISONS OF INDIVIDUAL TARGETS

3.1 RADIOMETRIC MODEL USING ECHOSIM PARAMETERS

We compare the radiometric model results using standard settings (as outlined in Table 2) and settings more akin to those of EChOSim (labelled as EChOSim QE & η in Table 2). Different sets of absolute noise floor levels with and without medium zodiacal light contribution are shown in Figure 3 and 4 for the cases of 55 Cnc e and GJ 1214b, respectively.

The effects of absolute noise floor level are undistinguishable in the case of the bright target (55 Cnc e), while it is only significant on the longer wavelengths for the faint target (GJ 1214 b). Zodi effect is only significant above ~5 μm.

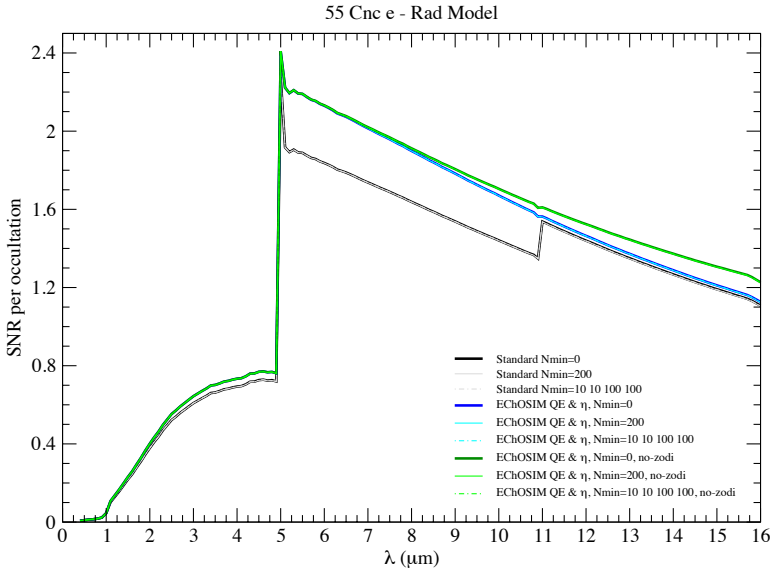

Figure 3. 55 Cnc e occultation. Black/Grey: Standard model assumptions (table 2) for Nmin = 0 / Nmin = 200. Blue: EChOSim throughput and QE (table 2). Green: No zodi contribution.

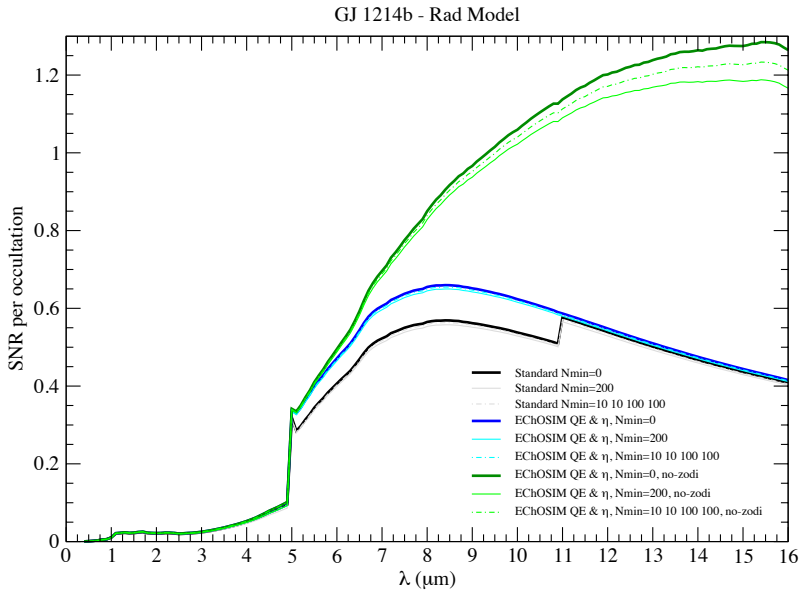

Figure 4. GJ 1214b occultation. Same legend as figure 2.

3.2 SUMMARY & DISCUSSION

In this section, we investigated the impact of running the ESA-RM with default parameters and with EChOSim quantum efficiencies and throughputs. We simulate the photon noise and background limted cases (as specified in the MRD), 55 Cnc e and GJ1214b, respectively.

Such simulations demonstrate the impact of varying system parameters on the final SNR of the spectrum. We found a ~20% gain in SNR for the wavelength range 5 – 11 μm when assuming the EChOSim parameters. There is no appreciable impact on the obtained SNRs otherwise.

There is no appreciable effect of the Nmin parameters for the photon noise limited case (55 Cnc e) and a small (at the few percent level) effect for the background limited case at long wavelengths.

4 RADIOMETRIC MODEL SNR VS ECHOSIM SNR

4.1.1 55 Cnc e

We first demonstrate the variation of EChOSim SNR given different assumptions. Figure 5 shows the SNR obtained with the standard version of EChOSim (with parameters given in Table 3) but with different thermal emission and zodiacal light settings. Zodi average and maximum levels are compared (in particular in the LWIR channel). The effect of thermal instrument emission (switched on in the standard model) is also shown, although changes are negligible.

We note that the differing morphologies of the SNR curves presented here are due to the different throughput assumptions of EChOSim and ESA-RM. EChOSim assumes a realistic dichroic chain (with wavelength dependent throughput, see figure 1) whilst ESA-RM assumes band wide constants. This results in a smooth SNR curve for the ESA-RM and to a more 'ragged' curve in the case of EChOSim.

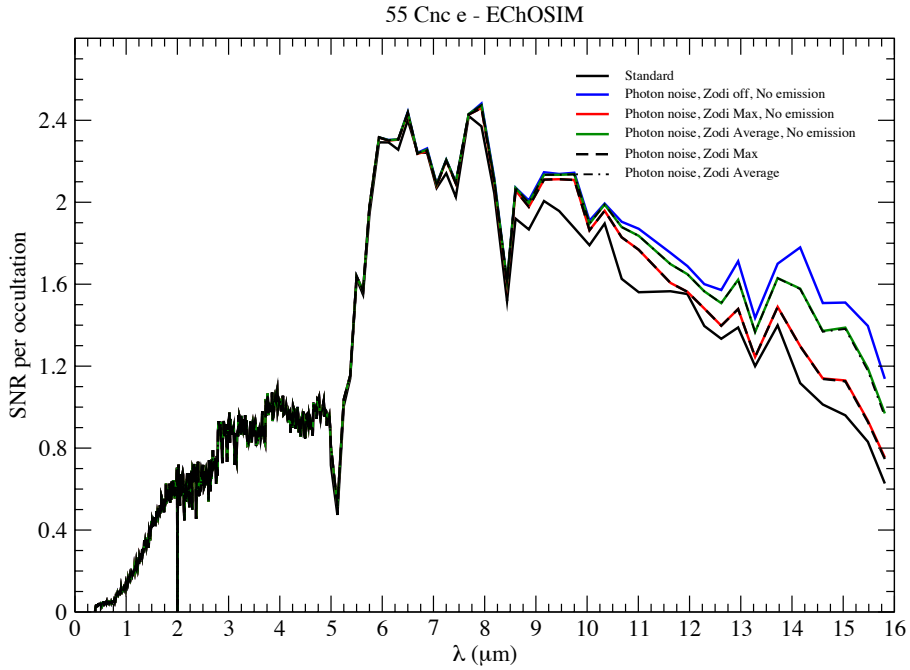

Figure 5. 55 Cnc e: Black continuous, standard setting (max. Zodi, thermal emission, full noise), black dashed, max Zodi setting (only photon noise), black dash-dotted, average zodi (only photon noise). Red, max Zodi, no instrument emission. Green, average Zodi, no instrument emission. Blue, no Zodi and no emission.

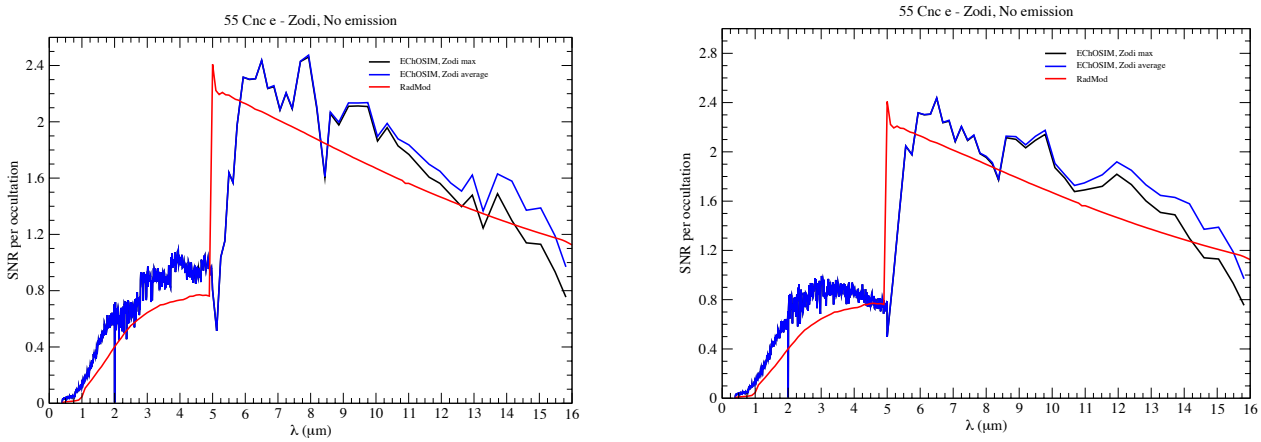

Figure 6. 55 Cnc e: Left, Method 2 binning, Right, Method 1 binning. Blue, EChOSim average Zodi. Black, EChOSim max Zodi. Red, ESA-RM (EChOSim QE and throughput and average zodi).

4.1.2 GJ1214b

Figure 7 shows the same results as Figure 5 for the case of the detector noise limited case (faint target, GJ 1214b). Here, Zodi level is important above 5 μm and thermal emissions is negligible. Figure 7 displays the SNR given by EChOSIM with standard parameters taking into account different noise sources. Readout noise is important in this case for longer wavelengths.

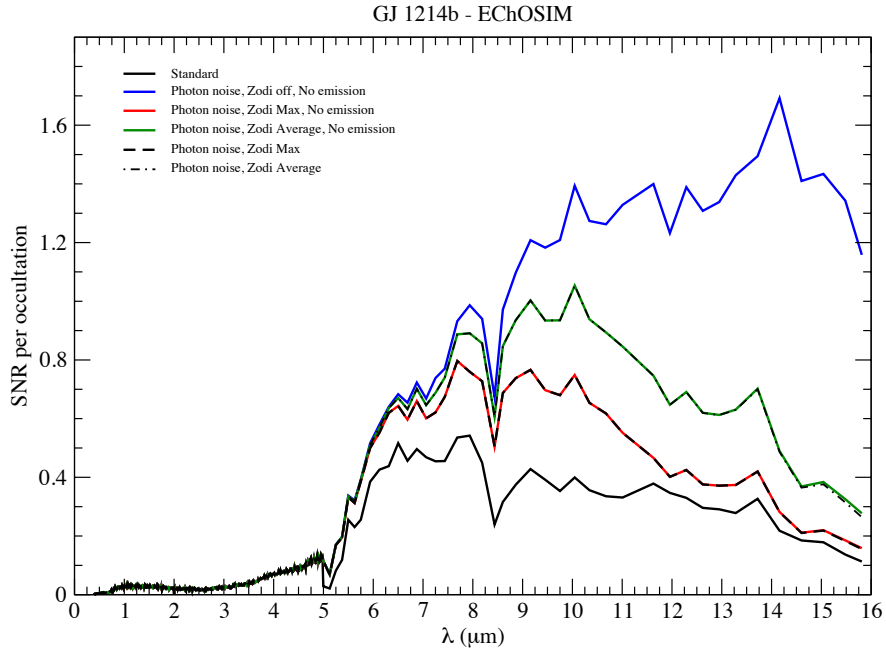

Figure 7. GJ1214b: Same description as figure 4.

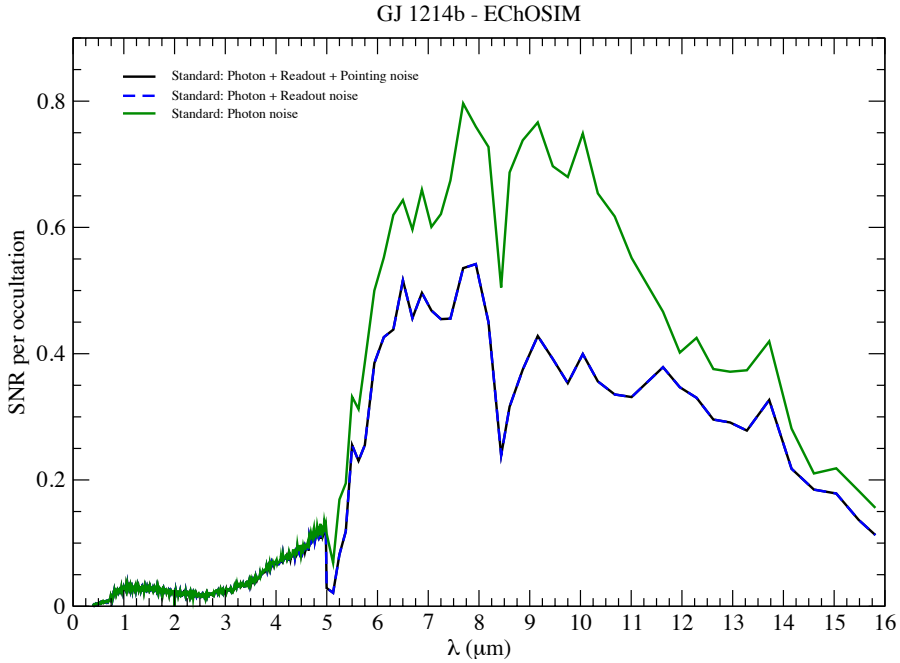

Figure 8. GJ1214b: Comparison of photon noise only case (green) to photon noise + read noise (blue) + pointing jitter noise (black). The 55 Cnc e equivalent plot is omitted since detector noise has a negligible impact in the photon-limited case.

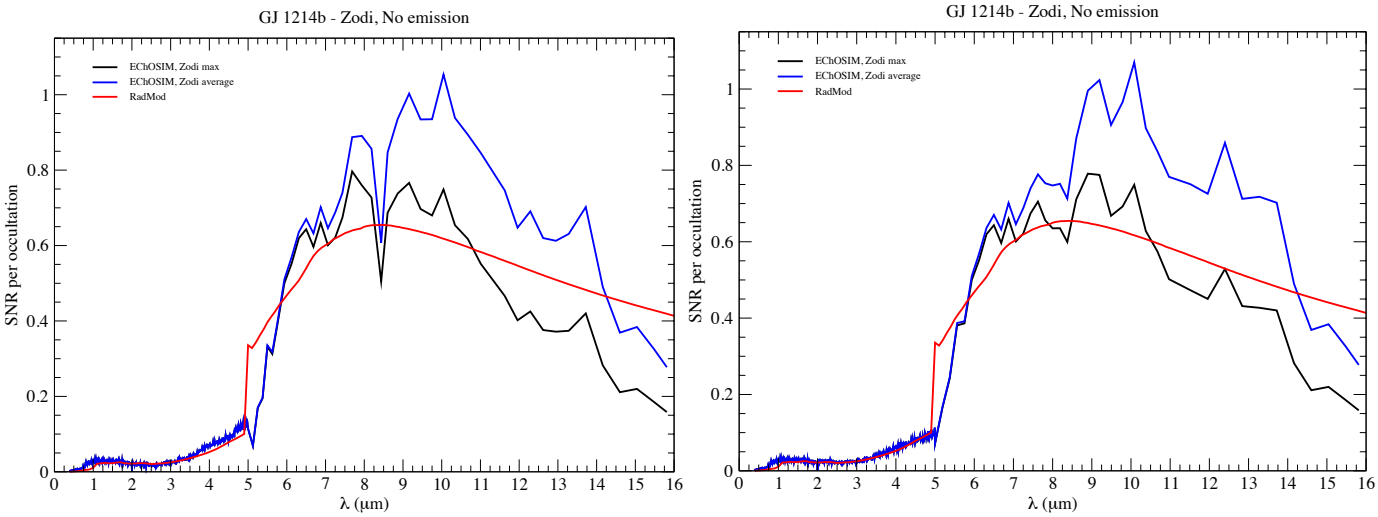

Figure 9. GJ1214b: Left, Method 2 binning, Right, Method 1 binning. Blue, EChOSim average Zodi. Black, EChOSim max Zodi. Red, ESA-RM (EChOSim QE and throughput). No thermal emissions are assumed for EChOSim and we assume average Zodi levels for the ESA-RM.

4.2 SUMMARY & DISCUSSION

In this section we directly compare EChOSim and the ESA-RM with one another using the two test cases 55 Cnc e and GJ1214b. Here we explore two aspects: 1) The agreement of the ESA-RM with EChOSim in terms of SNR per wavelength; 2) The impact of diffuse emissions (zodiacal light).

1) Figures 6 & 9 show a good agreement between EChOSim and ESA-RM SNRs across all wavelengths. Whilst ESA-RM SNRs are smooth across wavelength bands (due to static throughput assumptions), we observe a significantly more 'ragged' functional form for EChOSim (due to more realistic wavelength dependent throughputs assumed). In the case of 55 Cnc e (figure 6), we find EChOSim to perform ca 20% better in the 2-5 μm range. We note however that this behaviour is strongly dependent on the wavelength binning method used (see figure 6). No such behaviour is observed for GJ1214b (figure 9).

   Sharp drops in SNR (for the EChOSim simulations) are due to dichroic overlaps between individual channels (e.g. 8.5 μm). EChOSim does not yet optimally calibrate for these areas of lower transmission and these localised SNR decreases must hence be seen as 'worst case' assumptions.

2) In figures 5 & 7 we show the impact of zodiacal light on the SNR achieved by EChOSim for both test cases. As expected (and in concord with the ESA-RM behaviour in section 3) we observe negligible effect of zodi emissions below 5 μm for both cases. Diffuse emissions are more problematic for background limited targets (GJ1214b) than for the photon limited ones, as expected.

   Figure 8 show the impact of various noise sources on the final SNR of GJ1214b. For faint targets, fixed noise terms such as read-out noise are significant whilst noise due to pointing instabilities is negligible in these cases (see Pointing Jitter technote, in prep.).

5 COMPARISONS OVER MAGNITUDE RANGES

Assuming a given planet/star system, we have investigated SNR achieved over a range of *K*-band magnitudes for three characteristic systems: 1) hot-Jupiter orbiting a G0 stars, 2) hot-Neptune orbiting a K0 star and 4) a hot SuperEarth orbiting a M4 star. The goal is to check if there are differences on the SNR predicted by EChOSIM and ESA-RM as a function of the brightness of the target for different typical targets that will be observed. Throughout this section, ESA-RM with EChOSim QE & η parameters (listed on the second column in Table 2) and EChOSim standard parameters (listed in Table 3) are used. Average and maximum zodi levels are tested, although differences are only distinguishable above 5 μm.

5.1.1 Hot-Jupiters

In these simulations, a G0V star orbited by a hot-Jupiter was simulated. All orbital or stellar parameters were fixed and the stellar magnitude varied as only free parameter.

Figures 10*a* and *b* compare the SNR achieved by ESA-RM and EChOSim for varying Zodiacal light contributions.

There is good agreement between ESA-RM and EChOSim over all wavelength ranges and magnitudes. In the longer wavelengths, EChOSim is achieving a lower SNR than the ESA-RM calculated values for the faint targets (see discontinuous lines in bottom right plots in both figures 10a and 10b).

Comparing figures 10a and 10b demonstrates (as discussed in section 2.5) that the SNR achieved is sensitive to the binning employed. This is particularly true in the shorter wavelengths where the spectral resolving power is higher.

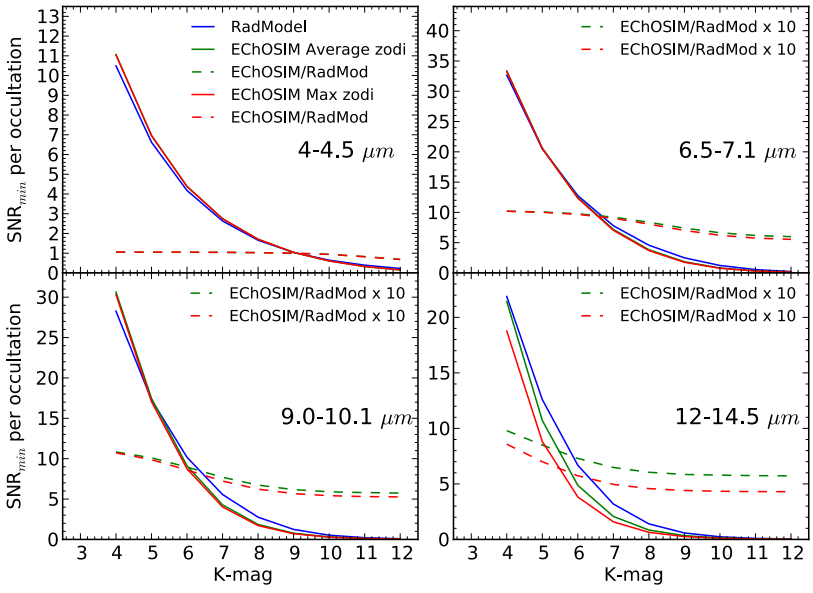

Figure 10a. SNR for a Hot Jupiter orbiting a G0 star; binning method 1. Blue: ESA-RM, Green: EChOSim (average zodi), Red: EChOSim (max. zodi), Green discontinuous: ratio (multiplied by a factor of 10 for clarity where indicated) of EChOSim (average zodi) to ESA-RM. Red discontinuous: ratio of EChOSim (max zodi) to ESA-RM.

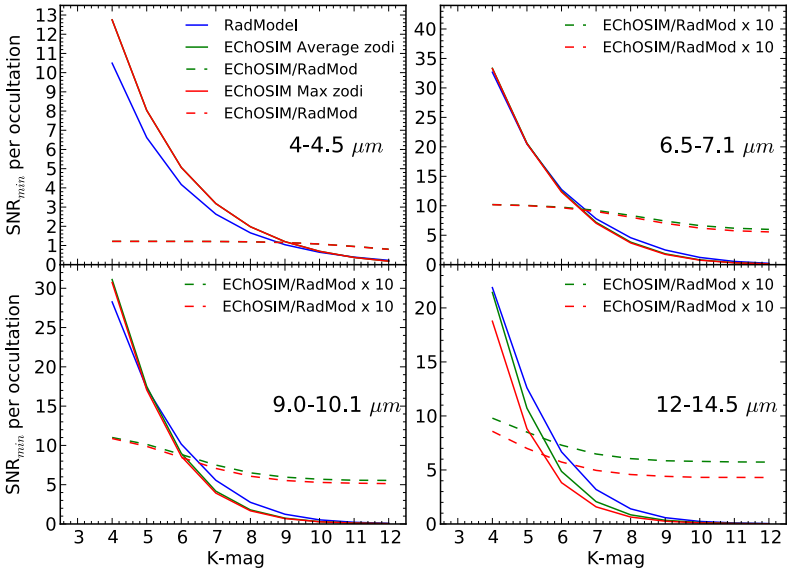

Figure 10b. SNR for a Hot Jupiter orbiting a G0 star; and method 2 binning. Otherwise same as figure 10a.

5.1.2 Hot-Neptunes

In these simulations, a K0V star orbited by a hot-Neptune was simulated. All orbital or stellar parameters were fixed and the stellar magnitude varied as only free parameter.

In figures 11a and 11b we see EChOSim performing slightly worse in terms of SNR achieved for the shorter wavelengths and faintest stars whist the opposite behaviour is true in the long wavelength channel where EChOSim performs marginally better for the brightest targets. For all other wavelengths and stars considered the SNRs obtained by both codes are in very close agreement with each other.

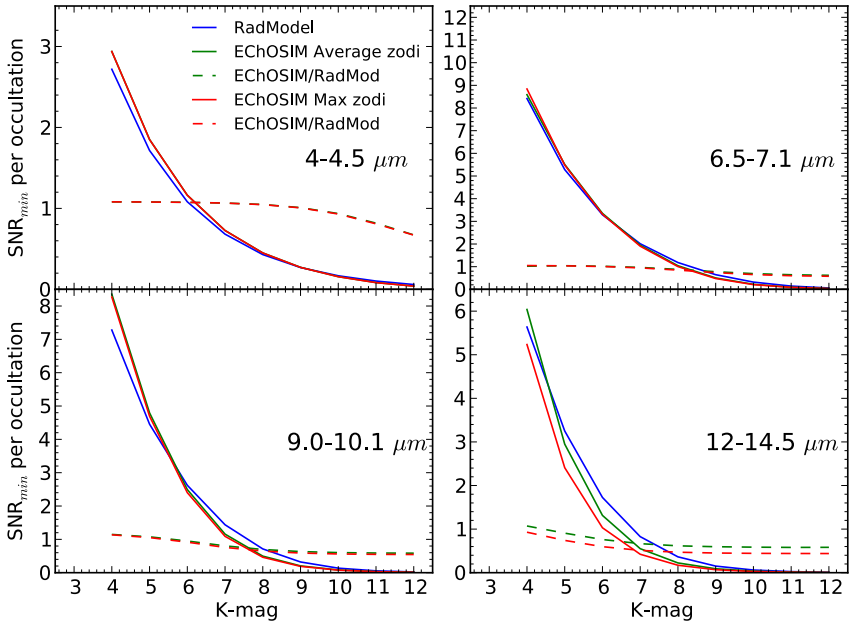

Figure 11a. SNR for a Hot Neptune orbiting a K0 star; binning method 1. Otherwise same labels as figure 10a.

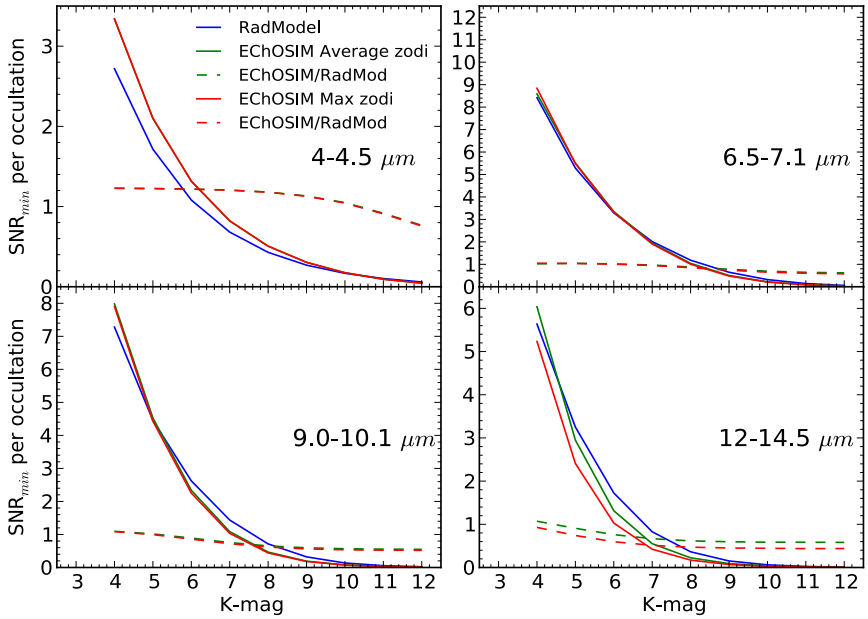

Figure 11b. SNR for a Hot Neptune orbiting a K0 star; binning method 2. Otherwise same labels as figure 10a.

5.1.3 Hot-SuperEarths

In this section, a M4V star orbited by a hot-SuperEarth was simulated. All orbital or stellar parameters were fixed and the stellar magnitude varied as only free parameter.

We find EChOSim and ESA-RM to be in excellent agreement for the shorter wavelengths whilst ESA-RM outperforms EChOSim in terms of SNR achieved for all other wavelengths for stars fainter than K-mag ~5, see figures 12a and 12b.

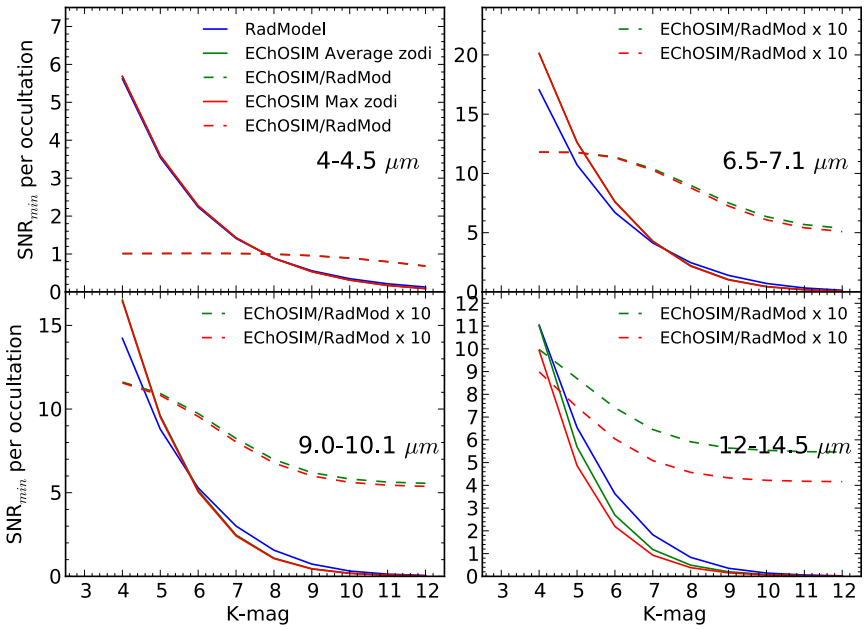

Figure 12a. SNR for a Hot Super-Earth orbiting a M4 star; binning method 1. Otherwise same as figure 10a.

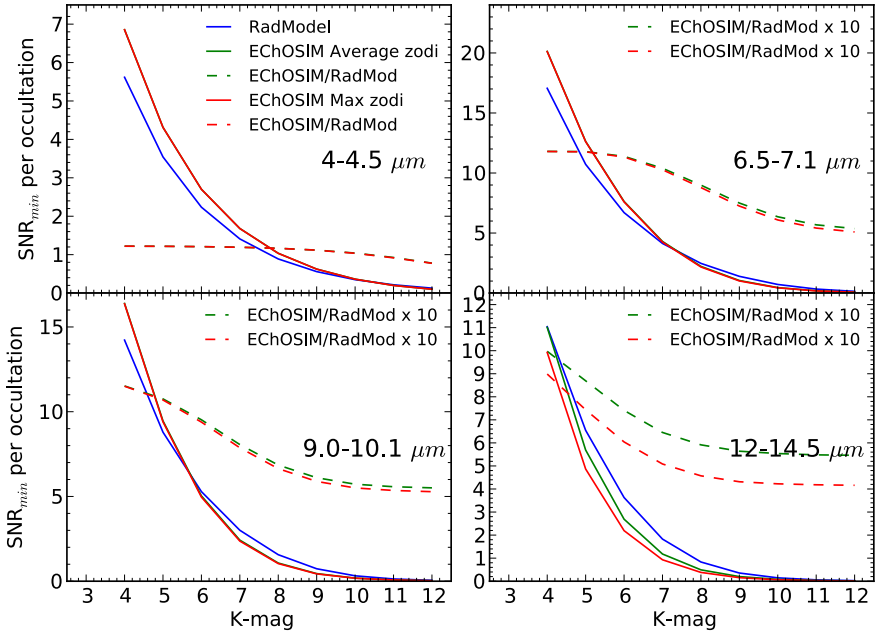

Figure 12b. SNR for a Hot Super-Earth orbiting a M4 star; binning method 2. Otherwise same as figure 10a.

5.2 SUMMARY & DISCUSSION

In this section we investigated the SNR variabilities of EChOSim and the ESA-RM for a variety of host stars and planet types as function of stellar brightness. For this, we have considered three planet-star systems: 1) G0 main sequence star orbited by a hot-Jupiter; 2) K0 main sequence star orbited by hot-Neptune; 3) M4 main sequence star orbited by a hot-SuperEarth. These cases span the observable range of EChO. Throughout the individual simulations, we kept all parameters fixed and only varied the host-star's brightness. The SNR vs K-mag plots are presented for each case study and for each binning method.

Results of individual simulations are briefly described for each case study in the previous section. The overall trends observed are two: 1) EChOSim yields slightly higher SNRs for very bright (K-mag = 4-5) targets and 2) performs worse by up to a factor of two compared to the ESA-RM for faint targets (K-mag > 8). This may be attributed to the fixed *Nmin* noise floor of the ESA-RM underestimating the actual noise contribution for the faint targets. These trends are strongly wavelength and case dependent (see figures in previous section).

Overall there is a good agreement between EChOSim and ESA-RM throughout this study.

6 SUMMARY, DISCUSSION AND CONCLUSION

In this tech note we compare the performance of EChOSim with that of the ESA Radiometric model.

For the comparison, we ran the ESA-RM using the standard model parameters (with the exception of Nmin as explained in the text), as well as model parameters that are more akin to those used by EChOSim.

With these two settings we proceed to comparing the ESA-RM and EChOSim using the two limiting cases identified in the MRD: 1) The photon limited case (planet: 55 Cnc e) and 2) the background limited case (planet: GJ 1214b).

In section 3, we investigated the impact of running the ESA-RM with default parameters and with EChOSim quantum efficiencies and throughputs. Such simulations demonstrate the impact of varying system parameters on the final SNR of the spectrum. We found a ~20% gain in SNR for the wavelength range 5 – 11 μm when assuming the EChOSim parameters. There is no appreciable impact on the obtained SNRs otherwise.

In section 4, we make a direct comparison between EChOSim and the ESA-RM for the photon noise limited and detector noise limited cases (as defined in the MRD), 55 Cnc e and GJ1214b, respectively. We furthermore explore the impact of different diffuse emissions (such as Zodi background), on the SNR of the retrieved spectrum. In these simulations we demonstrate that such effects are negligible in the shorter wavelengths (< 5 μm) but as expected are significant in the mid-IR.

Overall we find a good agreement between ESA-RM and EChOSim for the photon and background limited.

In section 5, we move away from the direct comparison using two test cases but investigate the SNR variabilities of EChOSim and the ESA-RM for a variety of host stars and planet types as function of stellar brightness. Such simulations show potential behavioural differences between ESA-RM and EChOSim with respect to the calculation of the astrophysical scene and in particular the host-star flux and Zodiacal background.

For a wide range of planet, star types and stellar magnitudes we find a good agreement between both ESA-RM and EChOSim.

Here we have demonstrated that EChOSim is in agreement with the ESA-RM in terms of SNR achieved under controlled conditions. As self-evident disclaimer, we would like to point out the limitations of such a study.

The ESA-RM and EChOSim are two very different models following two different philosophies. The ESA-RM is a static model using simplified assumptions (e.g. constant throughput per band, minimum absolute noise terms, etc.) with its design goal of ‘sizing the mission’. EChOSim is a fully dynamic end-to-end simulator from the astrophysical scene to a preliminary ground-based data reduction pipeline, encompassing a full simulation of the telescope and instruments. EChOSim’s design goal is to be an ‘as realistic as possible simulation of current engineering considerations’.

Given the very different nature of both codes, it is difficult to draw meaningful comparisons. Whilst shown to be in concord in controlled conditions, it is possible that results may (or in some cases should) vary given real life applications.